



HAL
open science

aDNA, ethnography, and facial approximations of the Teouma Lapita burials (c. 3000BP)

Susan Hayes, Hallie Buckley, Frédérique Valentin, Stuart Bedford, Matthew Spriggs

► **To cite this version:**

Susan Hayes, Hallie Buckley, Frédérique Valentin, Stuart Bedford, Matthew Spriggs. aDNA, ethnography, and facial approximations of the Teouma Lapita burials (c. 3000BP). *Journal of Archaeological Science*, 2024, 162, pp.105916. 10.1016/j.jas.2023.105916 . hal-04372013

HAL Id: hal-04372013

<https://hal.science/hal-04372013>

Submitted on 4 Jan 2024

HAL is a multi-disciplinary open access archive for the deposit and dissemination of scientific research documents, whether they are published or not. The documents may come from teaching and research institutions in France or abroad, or from public or private research centers.

L'archive ouverte pluridisciplinaire **HAL**, est destinée au dépôt et à la diffusion de documents scientifiques de niveau recherche, publiés ou non, émanant des établissements d'enseignement et de recherche français ou étrangers, des laboratoires publics ou privés.



aDNA, ethnography, and facial approximations of the Teouma Lapita burials (c. 3000BP)

Susan Hayes^{a,*}, Hallie R. Buckley^b, Frédérique Valentin^c, Stuart Bedford^{d,e}, Matthew Spriggs^{f,g}

^a Centre for Archaeological Science, Faculty of Science Medicine and Health, University of Wollongong, Australia

^b Department of Anatomy, Otago School of Biomedical Sciences, University of Otago, Dunedin, New Zealand

^c National Centre for Scientific Research (CNRS), UMR 8068, Nanterre, France

^d College of Asia and the Pacific, The Australian National University, Canberra, Australia

^e Department of Linguistic and Cultural Evolution, Max Planck Institute for the Science of Human History, Leipzig, Germany

^f School of Archaeology and Anthropology, College of Arts and Social Sciences, The Australian National University, Canberra, Australia

^g Vanuatu Cultural Centre, Port Vila, Vanuatu

ARTICLE INFO

Keywords:

Geometric morphometrics
Photographic averaging
Facial reconstruction
Vanuatu

ABSTRACT

Although ancient DNA (aDNA) cannot predict the facial appearance of skeletal human remains, knowing which extant populations are most closely related to the deceased has proven to be invaluable in rectifying two early facial approximations (popularly known as facial reconstruction) undertaken 15 years ago. These concerned two of the crania excavated from the Lapita burial site at Teouma on the island of Efate, and are associated with the first human arrival in the Vanuatu archipelago approximately 3000 years ago. This experimental revision to incorporate aDNA into both the methods and results has found there are advantages of knowing the genetic affiliation for estimating facial appearance. Specifically, we have found that this knowledge (i) facilitates identifying which of the current statistically valid predictors of the facial features are the most appropriate, (ii) informs the depiction of sexually dimorphic patterns of facial aging, and (iii) guides the portrayal of the subtle facial morphologies that fall outside what is currently provided by statistically validated skull-soft tissue algorithms and inter-relationships.

1. Introduction

The Teouma Lapita cemetery site on the south coast of Efate Island, Vanuatu was excavated from 2004 to 2010 (Bedford et al., 2006, 2009), and remains the largest cemetery yet found in the Western Pacific of this foundational Pacific Islands' culture. The first three field seasons (2004–2006) produced a number of skeletons without the skull in its anatomical orientation, although seven crania were recovered in secondary burials including one in a jar burial. In 2008, facial approximations (estimations of facial appearance) were completed of four of the newly reconstructed crania that had most of the facial bones preserved (B10A, B10B, B10C and B30A). This work was undertaken before the site had been securely dated, the analyses of the remains had only just begun, and the likely population affinities of the Teouma Lapita were unknown. The facial appearances were estimated following a method developed by Wilkinson (e.g., Needham, 2002) that combined the 2D techniques of Taylor (2001:373–404) with Neave's 3D anatomical

approach (Prag and Neave, 1997:29–30). The publication that presented the results (Hayes et al., 2009) was relatively brief regarding what methods were applied, with the main focus being the artistic advantages of manual sketching when dealing with partial remains (Fig. 1, top row).

In both images the individuals are, from left: B10A (male), B10B (female), B10C (male). This revision concerns B10A and B10B.

Subsequent research has resulted in the skeletal remains, including two secondarily displaced crania TeoQE (Teouma Quarry Edge) being directly radiocarbon dated to 3020–2740 cal. BP and genotyped (Lipson et al., 2018; Skoglund et al., 2016). All are estimated to be older adults (Buckley et al., 2008 and author's data). A first morphometric analysis of 5 of the 7 skulls indicated that these individuals are related to modern East Asian populations, contrary to what was expected in earlier studies (Valentin et al., 2016). Ancient DNA (aDNA) full genome analyses have more precisely shown that the remains are most closely related to modern populations from Taiwan (e.g., the Ami and Atayal) and the western Cordillera mountains of Luzon in the northern Philippines (e.g.,

* Corresponding author.

E-mail address: susan_hayes@uow.edu.au (S. Hayes).

<https://doi.org/10.1016/j.jas.2023.105916>

Received 3 August 2023; Received in revised form 30 November 2023; Accepted 4 December 2023

Available online 15 December 2023

0305-4403/© 2023 The Authors. Published by Elsevier Ltd. This is an open access article under the CC BY license (<http://creativecommons.org/licenses/by/4.0/>).

the Kankanaey), as well as to the skeletal remains of Tongan individuals dated to 2690-2320 cal. BP (Lipson et al., 2018; Lipson et al., 2020; Posth et al., 2018; Skoglund et al., 2016; and see Valentin et al., 2020 for dating of the Tongan individuals).

These aDNA studies point to a complex population dynamic suggesting at least two gene flows separated in time within the Pacific region, including an early move from East Asia and a later gene flow from North Melanesia. The Teouma remains, representative of the initial migration, are homogeneous in terms of nuclear and mitochondrial DNA (mtDNA), and for males the Y-chromosome haplotype, and display little Papuan admixture overall. See Supplementary Materials (SM) Table 1 for a summary of the mtDNA and Y-chromosome haplotypes of the Lapita-associated individuals, and SM Table 2 for the radiocarbon results.

Overall, these results and further aDNA studies in the Pacific, particularly those of East Polynesian and Micronesian populations, have gone a long way towards settling questions of the origins of Pacific peoples (Hudjashov et al., 2018; Liu et al., 2022). The early Lapita population coming into the region was an almost completely unadmixed Southern East Asian one, ultimately derived from the Neolithic populations of southern China (Huang et al., 2022; Yang et al., 2020). They leapfrogged from an early-established base in the Bismarck Archipelago past the main Solomon Islands chain to reach the Santa Cruz group and Vanuatu around 3000BP (Sheppard, 2019). The Teouma individuals were part of this earlier migration.

Subsequently, in the southern Remote Oceanic region (including Vanuatu, Fiji and the whole of Polynesia), a later migration of individuals identified as being genetically most like the present-day Papuan-speaking populations of New Britain – such as the Baining, again leapfrogged the main Solomons chain to join and subsequently to admix with the initial Southern East Asian population of Vanuatu and

adjacent archipelagos (Lipson et al., 2018; Posth et al., 2018). This secondary migration, following the same track as the earlier one, can be dated to the late or immediately post-Lapita period around 2500BP on the basis of only very slightly admixed Papuan individuals present in at least two different parts of Vanuatu at that time. Today's ni-Vanuatu populations are a mixture of these separate migrations and some later back-migration from Polynesia, with a Papuan genetic signature predominating (Lipson et al., 2020). In Western Polynesia an admixed population resulting from these two migrations was present by at least 1200-1000 BP, prior to the settlement of Eastern Polynesia, with the Southern East Asian signature predominating (Posth et al., 2018).

In 2022, the Deutsches Hygiene-Museum Dresden expressed an interest in displaying the original facial approximations in an exhibition concerning the impact of genetic research on previous historical interpretations (*Von Genen und Menschen: Wer wir sind und werden könnten*, 11 February – September 10, 2023). The decision to revisit the work carried out 15 years ago was twofold. First, there has been considerable progress in the availability of statistically validated skull-soft tissue relationships derived from extant populations to predict the facial appearance of archaeological remains (see, for example, a review by Hayes, 2016a), and second, in response to the exhibition's focus, to explore the extent to which the aDNA findings could be incorporated to enhance both the methods and results.

This paper presents experimental revisions of two of the Teouma Lapita crania: B10A, an older man, and B10B, an older woman (refer Fig. 1). The process involves applying geometric morphometrics to create population averages derived from early ethnographic photographs of the indigenous Ami and Atayal from Taiwan and Kankanaey related groups from the western mountains of Luzon. These data are then used to evaluate, and select from, a choice of peer reviewed methods for predicting the facial features, and to guide estimating



Fig. 1. Original estimations and the burial context of the Teouma Lapita crania.

Table 1
Estimations applied to original and revised facial appearances.

	Original	Revised
facial Soft Tissue Depths (fSTD)	Fischer's 1905 Papuan data from 2 males (as reproduced in Wilkinson, 2004:130)	Stephan's (2017) global weighted means, (range 1718–8519, median 7227 individuals)
Eyes	Globe and pupil in the orbital centre (e.g., Krogman, cited in Taylor, 2001:428) Iris diameter (Larrabee and Makielski, 1993) Lateral orbital projection (Stephan, 2002; Wilkinson and Mautner, 2003) Location of the canthi (Stewart, 1983) Influence of the morphology of the orbital bones (Gerasimov, 1955:39)	Either a superolateral globe orientation and location of the canthi (Stephan and Davidson, 2008; Stephan et al., 2009) or inferolateral globe orientation and location of the canthi (Kim et al., 2016) Iris diameter (Driessen et al., 2011) Lateral orbital projection (Stephan, 2002) Location of the malar tubercle (Stewart 1983) Gerasimov (1955:39) evaluated
Nose	Nose width, nose base, commencement of nasal tip, and wing height (Rynn, 2007) Relationship between the inferior border of the nasal aperture and nostril visibility (Wilkinson, 2004:169)	Either Rynn et al. (2010) or Chu et al. (2020) for the nasal width, base, length and tip; Rynn et al. (2010) for nasal wing height Wilkinson (2004:169) evaluated
Mouth	Mouth width and orientation (Stephan, 2003; Wilkinson et al., 2003) Upper lip height (Gerasimov, 1955:31) Lower lip height (George, 1993:224, 226)	Mouth width and location of the mouth corners (Stephan, 2003) Lip heights (Dias et al., 2016) Oral fissure and superior vermilion line (Mala and Veleminska, 2016)

population appropriate feature shapes not covered by the predictions, including sexually dimorphic patterns of facial aging.

As with the initial estimations, these revisions are 2D facial approximations. The methods are not automated, and therefore require considerable familiarity with the relevant hard and soft tissues as well as understanding the various algorithms to predict feature shapes. A 2D estimation does have the practical advantage of being able to be undertaken in reference to digital photographs – providing the lens-subject distance is at least 2.5m, which is when perspective distortion approximates 3% (Elišová and Krsek, 2007), and that calliper measurements are taken directly from the remains. However, while our revised facial approximations refer to the same digital photographs (and of necessity, given the remains have not yet been scanned), the process is achieved computer graphically, and with far greater control, using *Adobe Photoshop 2023* (v.24). The ability of this computer-graphic approach to predict a deceased individual's facial appearance has been statistically evaluated with both forensic (Hayes, 2016b; Hayes et al., 2019) and archaeological (Hayes et al., 2017) remains, and these evaluations – which indicate an acceptable level of reliability – are further elaborated in the Supplementary Materials.

2. Materials and methods

2.1. Images of the crania

The fragmented Lapita remains were reconstructed between 2005 and 2007 by FV while visiting the University of Otago (Valentin et al., 2016) in order to perform morphometric analyses. These were photographed for the facial approximations by Chris Smith (Curator, WD Trotter Museum, Anatomy Department, University of Otago) at a distance of ~2.5 m using a Nikon S24 (f/3.5, exposure 1/21 s, ISO-100, focal length 33 mm), with the focal point being the nasion (the midline intersection of the nasal and frontal bones). The relative

inexperience of SH and the fragility of the reconstructed remains led to not all of the photographs conforming to the Frankfurt Horizontal Plane (FHP): cranium B10C displays a slight head turn to the left, while skull B30A has a marked upwards head pitch, which was discussed in the ensuing publication (Hayes et al., 2009). This is why only the digital images depicting B10A and B10B (Fig. 2) were selected for the revision.

Top row B10A (male), bottom row B10B (female). Scale 50 mm.

2.2. Revised predictions of the facial feature shapes and positions

Table 1 summarises the previous and present predictive methods applied to estimate the facial appearance of B10A and B10B, which are discussed in more detail below. The facial feature predictions resulting from the algorithms and relationships that are to be evaluated in the light of the aDNA evidence are illustrated in Fig. 3, which, for added clarity, shows these in reference to outline traces of the crania illustrated in Fig. 3.

2.2.1. Facial Soft Tissue Depths (fSTD)

The facial Soft Tissue Depths (fSTD) originally applied were Fischer's 1905 Papuan data (as reproduced in Wilkinson, 2004), with this justified given the proximity to Vanuatu. In addition to the aDNA indicating little Papuan admixture, the Fischer 'means' are not statistically valid, being derived from two adult men. For this revision, Stephan's (2017) weighted means, calculated from global soft tissue depth studies reporting standard deviations (SD), were applied. The nine depths selected from this dataset are each derived from a large number of individuals (range 1718–8519, median 7227), which is much larger, and far more robust, than the small number of tissue depths reported from studies of specific population groups. Furthermore, given the differences in tissue depths due to a person's age, sex, body mass and population affinity are less than a measurement error of 10%, these weighted means have the advantage of being broadly applicable. In addition to applying an invalid dataset, the original orientations of the fSTDs were largely erroneous. Clarified in Stephan and Simpson (2008), not all fSTDs have a 'perpendicular' orientation, the angulation of some of the depths is dependent on the location of the corresponding soft tissue landmark, and in any event, 'perpendicular' in Aulsebrook et al. (1996) is the authors' shorthand for being at a right-angle to the bone tangent, and which, therefore, incorporates bone curvature. The definitions of the fSTDs and cranial landmarks applied in this revision are provided in SM Table 3, and illustrated in Fig. 3.

The estimated features on the left are from Stephan and Davidson (2008) for the placement of the eyes, and Rynn et al. (2010) for the nose, which are shown as blue lines on the left lateral view of the crania. Centre is Kim et al. (2016) for the eyes and Chu et al. (2020) for the nose, which are shown as green lines on the lateral crania. Each study's prediction of the start of the nasal tip is indicated by an open circle. The original identifications of the lateral palpebral ligaments (Stewart 1983) are indicated by a small red dot. The facial Soft Tissue Depths (fSTDs) and predictions for the mouth are the same for all. Scale 50 mm.

2.2.2. Eyes

The original estimations included a since invalidated recommendation that the globe and pupil are located within the centre of the orbit. A study of 375 adult Europeans scanned in a supine position (Guyomarc'h et al., 2012) has added validity to cadaveric studies indicating the globe is located superolaterally from the orbital centre (Stephan and Davidson, 2008; Stephan et al., 2009). However, a more recent study of 100 living, young adult Koreans scanned sitting upright with their head orientated in the standard anatomical position locates the centre of the pupil inferolaterally, with the authors suggesting their findings (which include validation) are related to the supine body orientation of the previous studies (Kim et al., 2016). Both methods for globe/pupil orientation are evaluated in this revision, including the locations for the palpebral ligaments. Unfortunately, the algorithm provided by Kim et al.

Table 2
Reference population multivariate regression results (n = 32, dependent variables PC1-6, cumulative variance 84%).

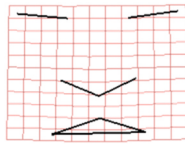
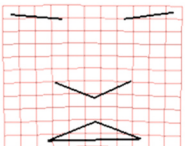
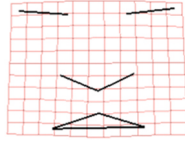
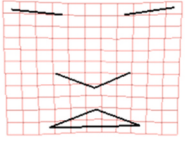
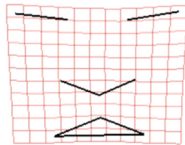
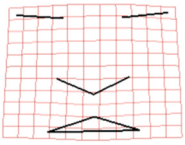
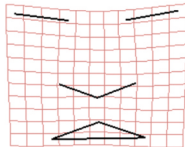
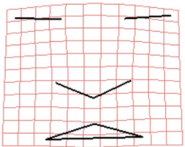
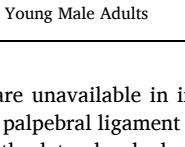
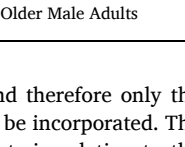
Variable	Multivariate regression statistics	Partial regression coefficients	Multivariate regression shape variance	
Island	Wilks' Lambda 0.76 F-Test 1.32 $p = 0.29$ (<i>n. sig</i>) PC 1-6 variance: 3.4% Total variance: 2.9%	PC2 14.8% variance Adj. $r^2 = 0.10$ $S = 0.008$ $p = 0.04$		
Sex	Wilks' Lambda 0.54 F-Test 3.54 $p = 0.01$ PC 1-6 variance: 12.4% Total variance: 10.4%	PC1 35.0% variance Adj. $r^2 = 0.21$ $S = 0.01$ $p = 0.004$	Taiwan 	Luzon 
Age	Wilks' Lambda 0.57 F-Test 3.13 $p = 0.02$ PC 1-6 variance: 6.4% Total variance: 7.5%	PC2 14.8% variance Adj. $r^2 = 0.22$ $S = 0.005$ $p = 0.004$	Men 	Women 
Age: Men (n = 12)	Wilks' Lambda 0.15 F-Test 4.49 $p = 0.06$ PC 1-6 variance: 11.6% Total variance: 12.3%	PC3 16.5% variance Adj. $r^2 = 0.30$ $S = 0.01$ $p = 0.04$	Young Adults 	Older Adults 
			Young Male Adults 	Older Male Adults 



Fig. 2. Frontal and left lateral images of the Teouma Lapita crania B10A and B10B.

relies on data that are unavailable in images, and therefore only the length of the medial palpebral ligament is able to be incorporated. The original location of the lateral palpebral ligaments in relation to the malar tubercle (Stewart, 1983) is retained (illustrated by a red dot in Fig. 3), but not the estimation of the medial in relation to the lacrimal fossa. As commented in Damas et al. (2020), while there is some agreement as to the width of the ligament, where it attaches varies considerably in the literature. Lateral orbital projection follows Stephan (2002), which is very similar to Wilkinson and Mautner (2003). The original incorporation of Gerasimov (1955:39) regarding the presence of epicanthic folds in Burial B10A is also evaluated in relation to the ethnographic images.

2.2.3. Nose

In 2008, Rynn's (at the time unpublished) algorithm for estimating the dimensions of the nose (Rynn et al., 2010) was applied. Although relatively reliable for Central European adults (Mala, 2013), Rynn's algorithms tend to be population specific, with modifications being required, for example, for Turkish (Bulut et al., 2019), and Japanese (Utsuno et al., 2016) adults. Sarilita et al. (2017) attempted to modify the algorithm for Indonesian adults, but found Rynn's original formulae performed better. This revision re-applies Rynn's algorithm to the Lapita remains but with a corrected identification of the subspinale (Caple and Stephan, 2015). A more recent approach devised by Chu et al. (2020) is also evaluated, using their equations to estimate nasal height, depth and location of the pronasale. Chu et al.'s regressions are derived from, and validated by, 240 medical CBCT scans and 3dMD photogrammetry taken from young adults living in north-western China. In addition, the

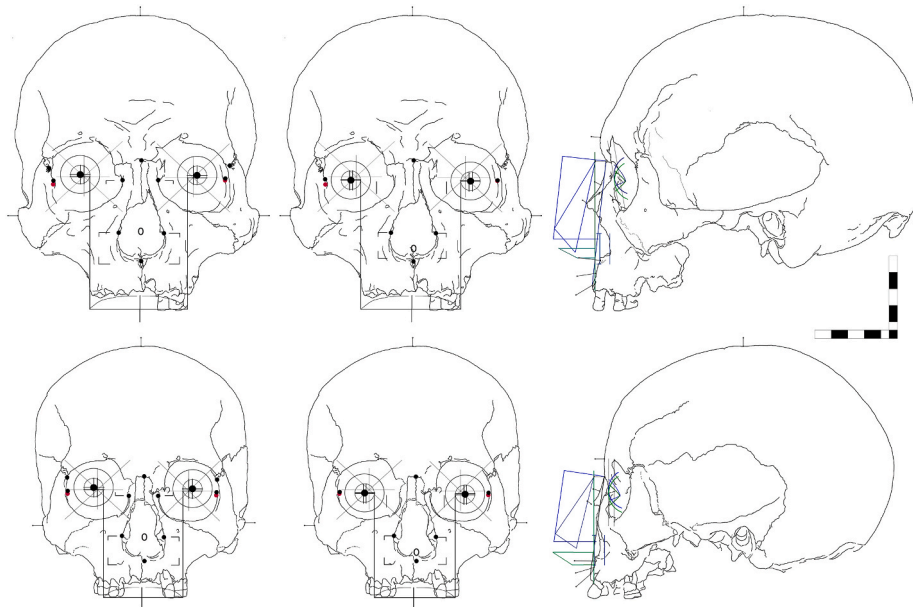


Fig. 3. Comparison of statistically verified feature estimations for B10A (top row) and B10B (bottom row).

relationship between the inferior border of the nasal aperture and nostril visibility, as described in Wilkinson (2004:169), is evaluated. The revision follows the original estimate of the likely location of Burial B10B's missing rhinion.

2.2.4. Mouth

In 2008 it was known that the mouth corners are close to the same vertical plane as the medial iris (Stephan, 2003), though this was impacted by both the invalidated globe position (e.g., Krogman, cited in Taylor, 2001:428) and incorrect iris width (Larrabee and Makielski, 1993). In the absence of the upper central incisors, the revision of the vermilion borders follows research that has found lip height to be ~26% of mouth width (Dias et al., 2016). Mala and Velemínska (2016) evaluated a number of studies of mouth prediction, and advise that the upper vermilion border is most accurately positioned near the upper quarter of the maxillary incisors and below the enamel boundary, and the oral fissure opposite the lower quarter of the maxillary incisors. For the Lapita revisions these locations are estimated from the preserved anterior teeth (left lateral incisor for Burial 10B, left lateral canine for Burial 10A), which, together with the evidence of tooth wear, make this an unavoidably highly approximate estimation. In the absence of the mandibular dentition, lower lip fullness is also highly approximate, and is not formally assessed.

2.3. Reference population images

As mentioned, the incorporation of aDNA into this revision involves directly referencing the facial variation of the populations most closely related to the remains. In 2022, when the work was undertaken, the main publication cited regarding the Teouma Lapita aDNA (Skoglund et al., 2016) only provided the Ami (also known as Amis), Atayal (also known as Tayal) and Kankanaey (also known as Kankana-ey, Kankanai) as examples of peoples from Taiwan and Luzon most closely affiliated with the Teouma Lapita individuals. However, to keep as close to the aDNA findings as possible, in late 2022 an online search of early ethnographic photographs (c. 1895–1930) yielded 32 digital images depicting 16 men and 16 women (population affinity and sex as described in the image captions) captured in a relatively frontal orientation: 16 are of the Ami and Atayal people and 16 are of people from Luzon that are recorded as members of the Kankanaey related groups from the western mountains. Of the images sourced, approximately half

were published online as sepia images, the remainder black and white. To facilitate blending in the production of the averages, all were converted to sepia in *Adobe Photoshop* (2023) (v.24). As can be seen in Fig. 4 (and refer SM Table 5), the images are balanced for island affinity (Taiwan, Luzon) and sex, though more varied with regards to estimations of age (young, mature, older adult), head pitch (up/down), and head turn (left/right).

Head pose (turn, pitch) and age (young, mature, older adult); refer SM Table 5 for the image codes.

The broader context for these ethnographic images is that most of the people appear to have been photographed outside, possibly positioned so as to be facing the sunlight. This may account for why the majority are depicted with their brows contracted. However, given the sociohistorical contexts of the image production, there are likely other factors in play that would cause many of the people to possibly appear ill at ease. Nearly all of the photographs of the Ami and Atayal people were taken shortly after the commencement of Japanese rule (1895), with at least one credited to the Japanese anthropologist Torii Ryūzō (see, for example F. Wong K, 2004). Some of the photographs from Luzon were taken shortly after the commencement of U.S. rule (1898), when a large number of Kankanaey people from the Northern Philippines (e.g., Bontoc, Suyoc) entered into employment contracts to perform in Western cultural expositions, commencing with the 1904 Louisiana Purchase Exhibition, which is also known as the St. Louis World's Fair (Afable, 2004; Buangan, 2004).

2.4. Geometric morphometric analyses

Each image was first digitised using the geometric morphometric software *tpsDig232* (Rohlf, 2015) with 60 landmark coordinates (26 homologous, 34 equidistant points) covering the face from brows to lower lip. These coordinates (Fig. 5, left) were used to produce statistical averages in the geometric morphometric software *tpsSuper32* (Rohlf, 2015), which outputs the average image with greater emphasis (darker) where the pixel intensities of the images in the dataset show stronger agreement. Refer to SM Table 6 for the landmark coordinate definitions.

Black dots are homologous, white are equidistant points. Left are the 60 coordinates applied to create the statistical averages and is the mean of the 16 reference images from Luzon. Right illustrates the 10 coordinates applied for the statistical analyses and is the mean of the 16 Taiwan reference population images.

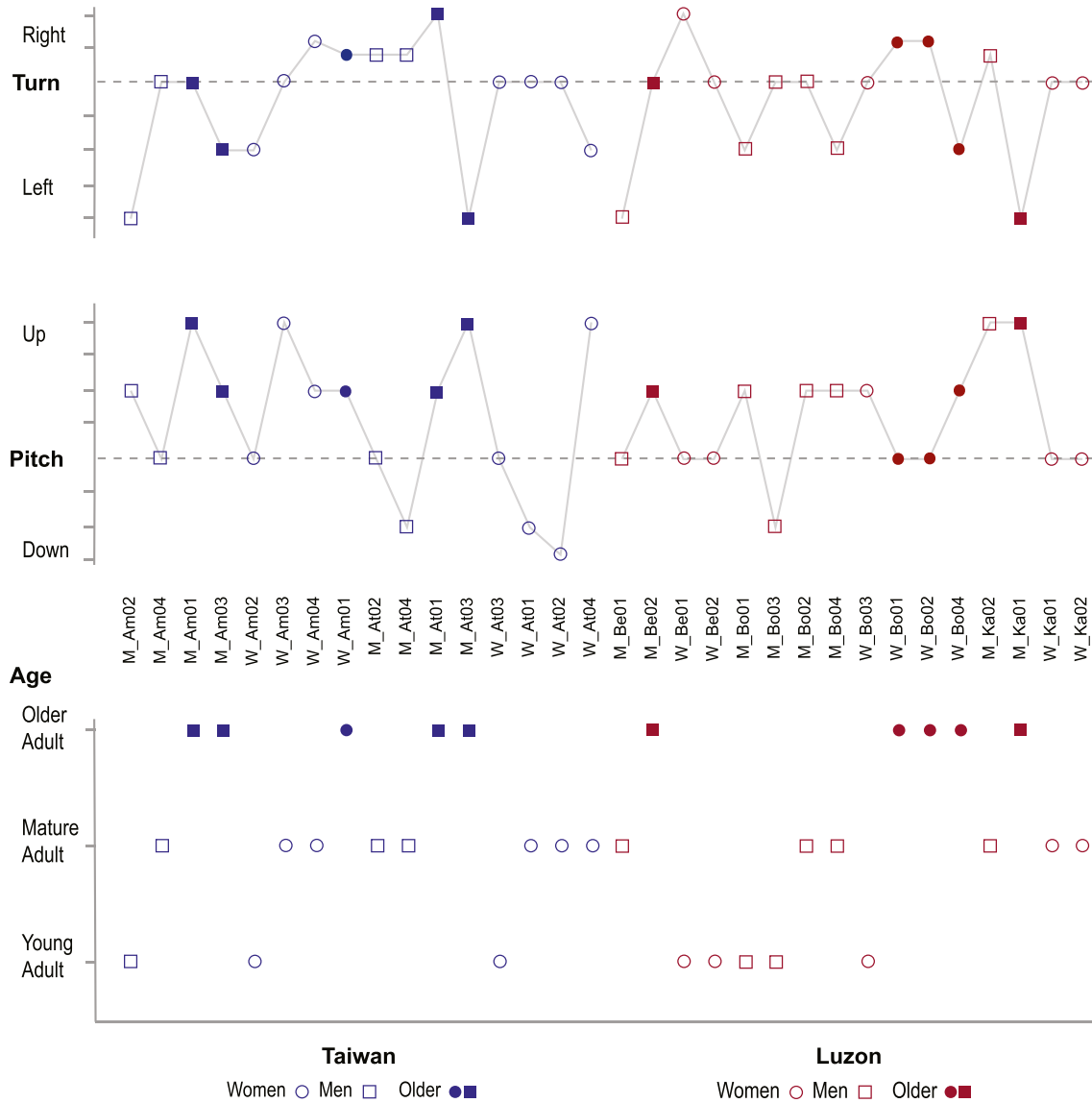


Fig. 4. Estimated reference population variation.

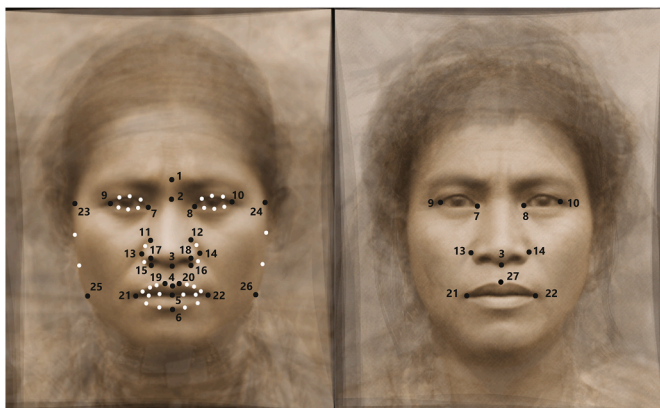


Fig. 5. Landmark coordinates.

There is a statistical requirement that the number of individuals in a dataset is greater than twice the number of landmarks if a multivariate regression (Goodall's F test) is undertaken. The formula is $N > (2k - 4) + (G - 1)$, where N is the number of individuals, k is the number of landmarks and G the number of groups (Webster and Sheets, 2010). Therefore, a sub-set of 10 coordinates capturing the main shape variance of the facial features relevant to the cranial landmarks (eye, nose and mouth widths, nose depth and upper lip fullness; Fig. 5, right) was applied to the 32 reference images. The multivariate regressions were undertaken in *morphologika2.5* (O'Higgins and Jones, 1998, 2006), and were to:

- (i) identify whether slight variations in head pose did not constitute a significant shape factor
- (ii) see if the reference images from both island population groups are of a sufficient similarity to be combined by sex and age
- (iii) identify indications of sexually dimorphic texture patterns relating to facial aging
- (iv) evaluate both the original and revised facial approximations in relation to the reference population images.

Following Procrustes registration (translated, scaled and rotated) in *morphologika2.5*, the multivariate regressions involving the reference images were undertaken with one independent variable (island, sex, estimated age) and the Principal Components (PCs) accounting for $\geq 80\%$ of the cumulative variance. The results (Wilks' Lambda, F-test, probability, variance) and partial regression coefficients (variance, adjusted r^2 , standard error, probability) were recorded, along with the wireframes and deformation grids indicating the shape variance arising from each regression. Identification of the variance within the individual PCs (Spearman's r_s) due to population affinity, sex, estimated age and head pose was undertaken with the statistical software *PAST4* (Hammer et al., 2001). A more general explanation of this approach to analysing digital images can be found in Hayes and Milne (2011).

2.5. Revised estimation of surface appearance

The different predictions for estimating the location and dimensions of the eyes and nose (refer Fig. 3) were superimposed over the reference population averages in *Adobe Photoshop* (2023) (v.24), with the averages calibrated to the width of the iris, which has a very low level of variance (Driessen et al., 2011). The predictions that were the most population appropriate (i.e., best agreed with the averages of the male and female features) were selected for revising the facial estimations. The selected predictions, and those applied to the original works, were digitised with the subset of 10 coordinates (refer Fig. 5, right), and multivariate regressions were undertaken in *morphologika2.5* with Lapita as the independent variable.

Estimating the surface appearance involved a base-line reference of the average of the 12 mature and older men and the average of 11 mature and older women using the geometric morphometric software *tpsSuper32* (refer to Section 2.4). Kyllonen and Monson (2020) recommend 12 images for averaging population specific age groups; however, the more recent research findings of Bülthoff and Zhao (2021) have been interpreted by Balas et al. (2023) as indicating facial averages of individuals of similar age, sex and population affinity attain relative stability with approximately 10–15 images. The resulting base-line reference population averages are illustrated in Fig. 6. For the revision, each of the average facial features (eyes, nose, mouth, outer face shape) was extracted and warped using the Transform feature in *Adobe Photoshop* (2023) (v.24) so as to fit both the selected predictions and the unique morphologies of the crania.

Photographic averages have been found to smooth the facial textures and therefore appear younger, which is an effect that increases with the number of images averaged (O'Toole et al., 1999), and is more marked with older individuals (Burt and Perrett, 1995). To counter this, clearer



Fig. 6. Average mature and older adults (60 landmarks) (left 12 men, right 11 women). The average facial features depicted here formed the baseline for the revised surface appearances, with each modified so as to agree with the predictive algorithms and the morphologies of the crania.



Fig. 7. Reference averages of older adults (60 landmarks) (left 5 men, right 4 women). The averages of the older adults were used to guide the depiction of mature aging in the revised facial approximations.

indication of mature facial aging was achieved by digital drawing, referring to the average of the oldest individuals (Fig. 7: 5 older men – without M_Ka01 due to an extensive facial tattoo – and 4 older women), as well as the sexually dimorphic patterns of facial aging indicated by the geometric morphometric analyses. Refer to Fig. 4 for the image data.

2.5.1. Illustrations of the lower face

The revisions necessarily focus on the upper head given the crania were not recovered with their associated mandibles. However, and for illustrative purposes only, an indication of the soft-tissue appearance of the lower face was accomplished by applying seven equidistant landmarks to the lower jaws of the older adult male, and female, reference population images. These were entered into *tpsSuper32* (refer to Section 2.4) to produce a statistical average, with each jaw vertically orientated to the estimation of the oral fissure, and warped using the Transform feature in *Adobe Photoshop* (2023) (v.24) so as to agree with the width of the estimated upper heads.

3. Results

3.1. Reference population image variance (10 landmark coordinates)

The PCA including the 32 reference population images results in estimated head pose attaining significance at very low variance values: head pitch PC8 (3.4% variance, $r_s = 0.48$, $p = 0.01$) and head turn PC9 (2.7% variance, $r_s = 0.49$, $p = 0.004$). Geometric morphometric analyses of images are highly sensitive to variations in head pose, but these results indicate that the slight variations across the images in head turn and pitch (refer to Fig. 4) have a minimal impact on the facial morphologies.

Table 2 summarises the results of the multivariate regressions with the independent variables of island (Taiwan, Luzon), sex and estimated age, and the dependent variables PC1–6, which account for 84% of the cumulative variance, and are relatively independent of the influence of head pose. As can be seen, both island affinity and estimated age have the same partial regression coefficient (PC2), indicating that the larger number of mature and older men in the Taiwan reference photographs (Fig. 4) may account for the Taiwan variance being similar to that of age and sex. However, and as can be seen in Table 2 (Age, $n = 12$), when the multivariate regression is balanced by male age (2 images of each age class per island, excluding images Am02, Am04, Bo02, Bo04), the shape variance is the same, with older men tending to have a higher inner eye corner, longer nose, and thinner upper lip. Therefore, with the full set of images, PC1 and PC2 account for most of the variance in sex and age, and, given the low level of shape variance between the two island populations, creating population averages that combine the two are

statistically justifiable.

Overall, and as illustrated in Table 2, the geometric morphometric multivariate regressions indicate that the sexual dimorphism of the reference population is that the women tend, on average, to have a shorter face height and fuller upper lip than the men, and that aging tends to result in a wider nose and a wider, thinner upper lip.

3.2. Best fit feature predictions with population averages

The different predictions for the locations and dimensions of the eyes, nose (and the same predictions for the mouth) of the Lapita crania – illustrated in Fig. 3 – are shown superimposed over the male reference population average ($n = 16$), and female reference population average ($n = 16$), in Fig. 8.

Positioning the eyes superolaterally (Stephan and Davidson, 2008; Stephan et al., 2009) generally agrees with the positions of the malar tubercles, which indicate the location of the outer eye corners (Stewart, 1983), and is a reasonable match for the lacrimal fossae indicating the inner eye corners. This prediction also agrees with the population averages in locating the tear trough terminating in the region of the inferior orbital rim (Sadick et al., 2007). The algorithms of Kim et al. (2016) predict a higher exocanthion than this reference population, locate the tear trough below the inferior orbital rim, and so may be more specific to the Korean population that was studied. Gerasimov's (1955:39) recommendation is that the orbital morphology of B10B would suggest an indication of an epicanthal fold. This is slightly present in some of the women depicted in the reference photographs, but at such a low frequency it is not marked in the statistical average.

The nose base, wing and commencement of the nasal tip predictions of Rynn et al. (2010) have a stronger agreement with the reference population averages, though the nose width prediction is an over-estimation for the average female. However, because the geometric morphometric analyses indicate that for both sexes the older individuals tend to have wider noses (refer Table 2), this width is likely acceptable for the Lapita remains. Chu et al. (2020) tend to locate the nasal base higher on the face and predict a narrower nose than the average of the men. This may be, however, due to the algorithms – as with Kim et al. (2016) – being derived from young adults. Wilkinson's (2004:169) recommendation that nasal guttering is associated with nostrils being visible in the Frankfurt Horizontal Plane appears to hold for the

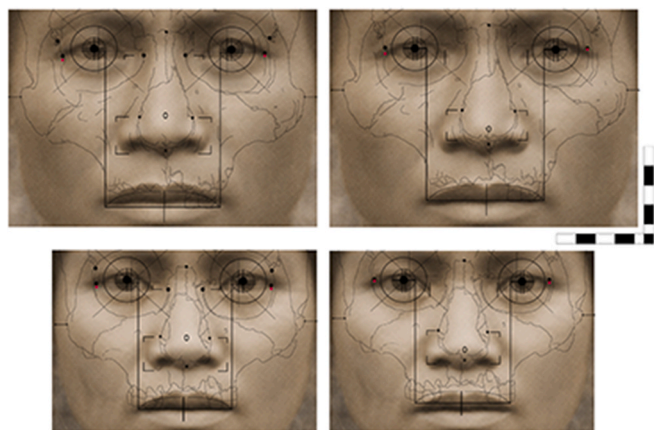


Fig. 8. Superimposition of the crania and feature predictions over the reference population averages. The predictions of Stephan and Davidson (2008) for the eyes, and Rynn et al. (2010) for the nose are shown on the left, right is the predictions of Kim et al. (2016) for the eyes and Chu et al. (2020) for the nose. Top row: superimposition of the two sets of predictions for the B10A crania over the male reference population average. Bottom row is the superimposition of the predictions for the B10B crania over the female reference population average. The averages are scaled to the diameter of the iris. Scale 50 mm.

reference population averages and all of the individuals who comprise them.

Upper lip height estimation (Dias et al., 2016) fits the male average, but underestimates the average woman's height, and foreshortens the height of the lower lip for both sexes. Locating the mouth corners on the same vertical plane as the medial iris (Stephan, 2003) is in reasonable agreement with both averages. Positioning the oral fissure at the incisal edge of the most anterior *in situ* teeth is highly approximate, as is the prediction that the upper vermilion line is on or below the enamel of the preserved anterior teeth (Mala and Velemínska, 2016).

When the best fit predictions for the eyes and nose (Rynn et al., 2010; Stephan and Davidson, 2008; Stephan et al., 2009) and the predictions for the mouth are digitised with the subset of 10 landmark coordinates and entered into *morphologika2*, the revised Lapita estimations are not statistically different from the 32 reference population images (independent variable Lapita, PC1-6, 84% cumulative variance: Wilk's Lambda 0.80, F-test 1.16, $p = 0.36$), and account for 2.7% of the total variation. Repeating this analysis with the original Lapita estimations is also insignificant (PC1-6, 84% cumulative variance: Wilk's Lambda 0.90, F-test 0.49, $p = 0.81$), and accounts for 1.65% of the variation.

Fig. 9 plots the results of PC1 (35% variance) and PC2 (14% variance), which are, respectively, significant for sex ($r_s = 0.46$, $p = 0.005$) and age ($r_s = 0.51$, $p = 0.002$) when both the original and revised Lapita estimations are entered into the analysis and evaluated. As can be seen, the Lapita revisions are located within the upper right quadrant, with B10A clustering with the older men, and Burial B10B with the older women. The original estimations of B10A and B10B, however, have higher scores for their respective sex (PC1, male = negative, female = positive), and both have lower values for age (PC2, older = positive, younger = negative).

The revised estimated upper faces for B10A and B10B are illustrated in Fig. 10, with and without the outlines of the crania and best fit predictions. These predictions are those located on the left of Fig. 3.

4. Discussion

Research into the effect of genetics on predicting facial appearance is progressing, but to date has limited practical application. Only a few genes have been reliably identified, the genetic inter-relationships are highly complex, and there has been low agreement across various studies in facial feature definition (Claes et al., 2018; Richmond et al., 2018). However, what genetics can more reliably predict is population ancestry, which, as demonstrated in this study, is invaluable for estimating the facial appearance of archaeological remains.

In 2008, the likely population affinities of Lapita people were contested unknowns (Pietrusewsky, 1996; Spriggs, 1997:99–107), the crania reconstructions were newly completed, and the remains had not been extensively analysed. Further, verified methods to estimate facial appearance were few, and most that were originally applied to the Teouma Lapita burials have since been invalidated (refer to Table 1). Although there are still considerable gaps in what can be predicted from human crania, over a period of 15 years this has evolved from being a narrow selection of (mostly) erroneous recommendations to a choice of statistically validated methods for estimating the same facial feature.

As noted earlier, the aDNA extracted from the Teouma Lapita remains (including Burials B10A and B10B), indicates these individuals are most closely related to extant populations from Taiwan (e.g., the Ami and Atayal) and from the Philippine Cordillera mountainous region of western Luzon (most particularly, the Kankanaey) (Lipson et al., 2018; Skoglund et al., 2016). Early photographs depicting these indigenous peoples were sourced, on the assumption that admixtures were likely less frequent a century ago. Statistical shape analyses (geometric morphometrics) of the facial features indicate that slight head pose variations in the photographs do not significantly impact the facial features, the two island populations are not significantly morphologically distinct, and therefore the full dataset of 32 men and women could be

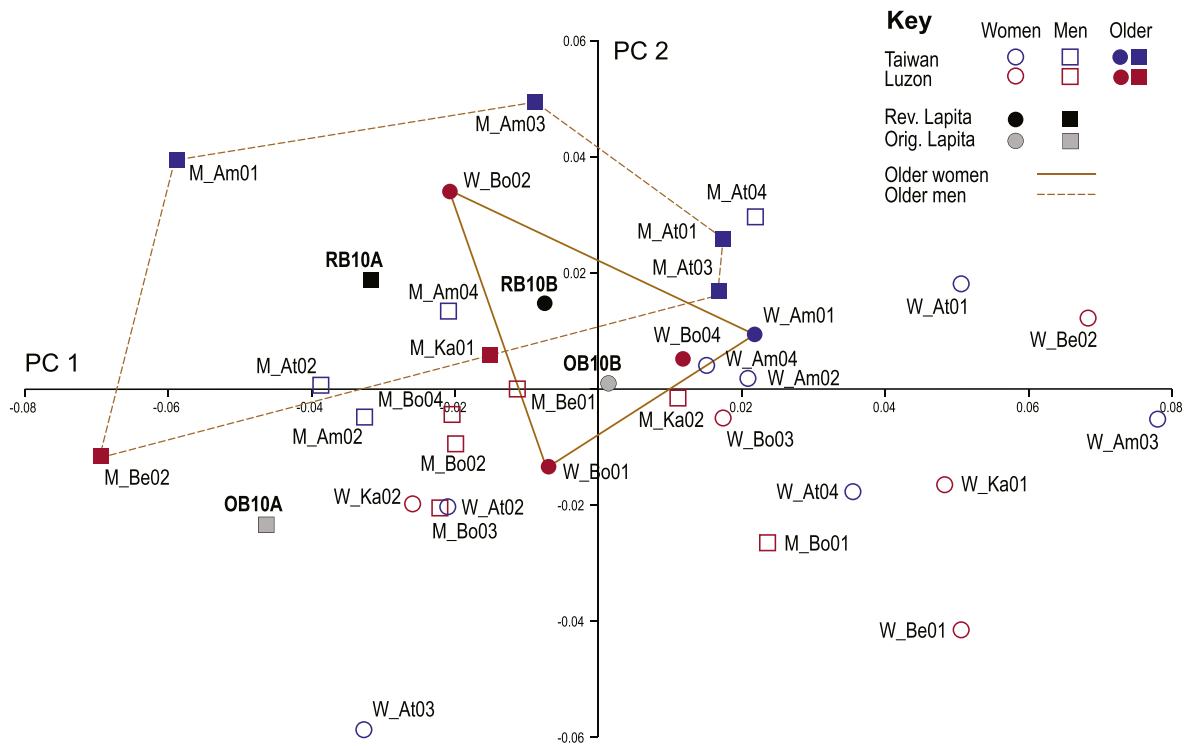


Fig. 9. Assessment of the Lapita estimations (original and revised) in the context of the reference population images. PC1 is significant for sex (female positive, male negative values) and PC2 is significant for age (older positive, younger negative values).



Fig. 10. Revised surface appearance of B10A (left) and B10B (right). The upper row illustrates the revisions at 90% transparency, superimposed with the cranial outlines and predictors used to estimate the facial appearances. Scale 50 mm.

used to (i) identify broad patterns of sexual dimorphism and facial aging, (ii) produce statistical averages, (iii) apply these findings to evaluate a selection of verified predictive methods for estimating the eyes and nose, (iv) achieve revised estimations of the surface appearances that are more population, sex and age appropriate, and (v) assess the overall differences between the initial and revised facial estimations.

Unexpectedly, when applied to the Lapita remains, the predictions derived from Western European adults have, overall, the strongest agreement with the reference population averages: Stephan and Davidson (2008); Stephan et al. (2009) for the eyes, and Rynn et al. (2010) for the nose. Likely contributing to this result is that both Kim et al. (2016) and Chu et al. (2020) present algorithms exclusively derived from young adults, which could impact their relevance to mature and older adult faces. Overall, the revised predictions of the feature locations and dimensions locate B10A and B10B within the variance of the reference population older men and women, while the largely invalidated relationships used to create the original estimations result in younger faces with a higher level of sexual dimorphism (refer Fig. 9).

Using facial averages to estimate the surface appearance is not new to facial approximation, though, as Vandermeulen et al. (2012:215) note, an average comprised of too few individuals will likely cause model bias (unwanted features are retained), while averages comprised of too many tend to be non-specific. The approach taken here is more targeted (refer to Fig. 6). The surface appearances refer to the average facial features of population appropriate mature and older individuals (12 men, 11 women), with the data being within the range of stability (10–15 images) for producing averages by age, population affinity and sex (Balas et al., 2023; Bühlhoff and Zhao, 2021; Kyllonen and Monson, 2020). The individual facial feature morphologies contained in these base-line averages (refer to Fig. 7) were warped using the Transform feature in Adobe Photoshop (2023) (v.24). These transformations were piecemeal, so as to agree with both the best-fit predictions and the unique morphologies of the crania, and with the geometric morphometric results indicating population relevant patterns of sexual dimorphism and mature aging. Reference averages derived from the older reference population individuals (5 men, 4 women; Fig. 8) were used to guide elements of digital drawing in order to counter the tendency for photographic averages to be judged younger than the images from which they were derived (Burt and Perrett, 1995; O’Toole et al., 1999).

In addition to providing an indication of population variation and a

way to evaluate predictive method suitability, aDNA may also help facial approximation practitioners avoid bestowing the deceased with their own facial characteristics, as documented in forensic applications by Taylor (2001:85–86). While unintended self-portraiture is likely related to the high level of unknowns in facial approximations, such impositions occur in depictions drawn from life. Gombrich (1982:132–133) describes “the puzzling obtrusion of the artist’s own likeness” onto the portrait they produce, and that this is more prevalent with the mouth and jaw. When the facial appearances of the Teouma Lapita remains were first estimated, inexperience and the application of invalid and erroneous predictions likely combined with manual sketching to result in some of the facial features having a Western European inflection – particularly with the curvature of the upper lip (Fig. 1, top row). There are ethical issues with colonial photographic practices (e.g., Salvador-Amores, 2016), but having access to a set of reference population averages has helped retain, rather than overwrite, the subtle facial morphologies that are common to a particular people, and this is particularly important when the practitioner does not share the population affinity of the deceased.

Finally, in our original publication (Hayes et al., 2009) we argued that including an estimated jaw was not justifiable, and this still holds. However, and for purely illustrative purposes, referring to the reference population images enables a depiction of B10A and B10B with, respectively, the average lower jaw of an older male and older female (Fig. 11).

5. Conclusions

Revisiting the facial approximations of the Teouma Lapita individuals in the light of more recently available aDNA evidence has been instructive. There is no doubt that aDNA has had a massive impact on archaeological interpretation in general, and particularly in the area of migration studies. Meanwhile, 15 years have passed since the earlier attempt at putting a face to the Lapita name, and this field of research has also advanced considerably, not least in the number of statistically valid predictions for the facial features. Adding all these developments together has led to improved estimations of the Lapita people’s facial appearance. However, while these revised estimations deploy a suite of statistically validated predictions and adhere to both the unique shapes of the Lapita crania and the average morphological characteristics of past peoples most closely related to them, the results are, of necessity, predominantly applications of statistical averages of human craniofacial variation and can never be viewed as exact portraits of the past.

Ethical statement

The authors acknowledge that their reference to historical photographs has ethical concerns. Although some of the photographs are documented in the literature as being taken as part of a contractual arrangement, and therefore presumably with informed consent, this would not have been the case for all. It is for this reason that none of the individuals photographed are depicted in our study.

Funding

This research did not receive any specific grant from funding agencies in the public, commercial, or not-for-profit sectors.

CRediT authorship contribution statement

Susan Hayes: undertook the data collection, Formal analysis, wrote the initial draft of the paper. **Hallie R. Buckley:** wrote the initial draft of the paper. **Frédérique Valentin:** provided additional information, editing and advice. **Stuart Bedford:** provided additional information, editing and advice. **Matthew Spriggs:** wrote the initial draft of the paper.



Fig. 11. Revised surface appearance of B10A (left) and B10B (right) with average lower jaw. Scale 50 mm.

Declaration of competing interest

The authors declare that they have no known competing financial interests or personal relationships that could have appeared to influence the work reported.

Acknowledgements

Our thanks to the Landowners, Chiefs and people of Eratap village, Efate, Vanuatu for their permission, collaboration and interest in the Teouma excavation project, especially Vanuatu Kaljoral Senta (VKS) filwoka Silas Alben. The lessee, Mr Robert Monvoisin is also thanked for allowing access to the site and other material support. Further general project acknowledgements can be found the various publications resulting from it. We would also like to thank Isabel Matthäus of the Deutsches-Hygiene Museum, Dresden, who approached MS and the VKS to invite participation in the Exhibition, and Viktoria Krason for liaising with SH regarding the Museum’s display of both the original and revised facial approximations. Our thanks also to the two anonymous reviewers whose thoughtful suggestions have improved the clarity of this paper.

Appendix A. Supplementary data

Supplementary data to this article can be found online at <https://doi.org/10.1016/j.jas.2023.105916>.

References

- Afable, P.O., 2004. Journeys from Bontoc to the western fairs, 1904-1915: the “Nikimalika” and their interpreters. *Philippine Stud.* 445–473.
- Aulsebrook, W., Becker, P., Yagar, M., 1996. Facial soft-tissue thicknesses in the adult male Zulu. *Forensic Sci. Int.* 79 (2), 83–102. [https://doi.org/10.1016/0379-0738\(96\)01893-2](https://doi.org/10.1016/0379-0738(96)01893-2).
- Balas, B., Sandford, A., Ritchie, K., 2023. Not the norm: face likeness is not the same as similarity to familiar face prototypes. *i-Perception* 14 (3). <https://doi.org/10.1177/20416695231171355>.
- Bedford, S., Spriggs, M.J.T., Regenvanu, R., 2006. The Teouma Lapita site and the early human settlement of the Pacific Islands. *Antiquity* 80 (310), 812–828. <https://doi.org/10.1017/S0003598X00094448>.
- Bedford, S., Spriggs, M., Buckley, H.R., Valentin, F., Regenvanu, R., 2009. The Teouma Lapita site, South Efate, Vanuatu: a summary of three field seasons (2004-2006). In: Sheppard, P., Thomas, T., Summerhayes, G. (Eds.), *New Zealand Archaeological Association Monograph, Lapita: Ancestors and Descendants*, vol. 28, pp. 215–234.
- Buangan, A.S., 2004. The Suyoc people who went to St. Louis 100 years ago: the search for my ancestors. *Philippine Stud.* 474–498.
- Buckley, H.R., Tayles, N.G., Spriggs, M.J.T., Bedford, S., 2008. A preliminary report on health and disease in early Lapita skeletons, Vanuatu: possible biological costs of island colonization. *J. I. Coast Archaeol.* 3 (1), 87–114. <https://doi.org/10.1080/15564890801928300>.
- Bülthoff, I., Zhao, M., 2021. Average faces: how does the averaging process change faces physically and perceptually? *Cognition* 216, 104867. <https://doi.org/10.1016/j.cognition.2021.104867>.

- Bulut, O., Liu, C.-Y.J., Gurcan, S., Hekimoglu, B., 2019. Prediction of nasal morphology in facial reconstruction: validation and recalibration of the Rynn method. *Leg. Med.* 40, 26–31. <https://doi.org/10.1016/j.legalmed.2019.07.002>.
- Burt, D.M., Perrett, D.I., 1995. Perception of age in adult Caucasian male faces: computer graphic manipulation of shape and colour information. *Proc. Roy. Soc. Lond. B259* (1355), 137–143. <https://doi.org/10.1098/rspb.1995.0021>.
- Caple, J., Stephan, C.N., 2015. A standardized nomenclature for craniofacial and facial anthropometry. *Int. J. Leg. Med.* 130 (3), 1–17. <https://doi.org/10.1007/s00414-015-1292-1>.
- Chu, G., Zhao, J.-m., Han, M.-q., Mou, Q.-n., Ji, L.-l., Zhou, H., Chen, T., Du, S.-y., Guo, Y.-c., 2020. Three-dimensional prediction of nose morphology in Chinese young adults: a pilot study combining cone-beam computed tomography and 3dMD photogrammetry system. *Int. J. Leg. Med.* 134 (5), 1803–1816. <https://doi.org/10.1007/s00414-020-02351-8>.
- Claes, P., Roosenboom, J., White, J.D., Swigit, T., Sero, D., Li, J., Lee, M.K., Zaidi, A., Mattern, B.C., Liebowitz, C., 2018. Genome-wide mapping of global-to-local genetic effects on human facial shape. *Nat. Genet.* 50 (3), 414–423. <https://doi.org/10.1038/s41588-018-0057-4>.
- Damas, S., Cordón, O., Ibáñez, O., 2020. Relationships between the skull and the face for forensic Craniofacial Superimposition. In: *Handbook on Craniofacial Superimposition*. Springer, pp. 11–50. https://doi.org/10.1007/978-3-319-11137-7_3.
- Dias, P.E.M., Miranda, G.E., Beaini, T.L., Melani, R.F.H., 2016. Practical application of anatomy of the oral cavity in forensic facial reconstruction. *PLoS One* 11 (9), e0162732. <https://doi.org/10.1371/journal.pone.0162732>.
- Diessen, J.P., Vuyk, H., Borgstein, J., 2011. New insights into facial anthropometry in digital photographs using iris dependent calibration. *Int. J. Pediatr. Otorhinolaryngol.* 75 (4), 579–584. <https://doi.org/10.1016/j.ijporl.2011.01.023>.
- Elišová, H., Krsek, P., 2007. Superimposition and projective transformation of 3D object. *Forensic Sci. Int.* 167 (2), 146–153. <https://doi.org/10.1016/j.forsciint.2006.06.062>.
- George, R.M., 1993. Anatomical and artistic guidelines for forensic facial reconstruction. In: *Iscan, M.Y., Helmer, R.P. (Eds.), Forensic Analysis of the Skull: Craniofacial Analysis, Reconstruction, and Identification*. Wiley-Liss, pp. 215–227.
- Gerasimov, M.M., 1955. *The Reconstruction of the Face from the Basic Structure of the Skull* (W. Tschernozky, Trans.). Nauka.
- Gombrich, E.H., 1982. The mask and the face: the perception of physiognomic likeness in life and art. In: *The Image and the Eye: Further Studies in the Psychology of Pictorial Representation*, pp. 105–136. Phaidon.
- Guymarc'h, P., Dutailly, B., Couture, C., Coqueugniot, H., 2012. Anatomical placement of the human eyeball in the orbit - validation using CT Scans of living adults and prediction for facial approximation. *J. Forensic Sci.* 57 (57), 1271–1275. <https://doi.org/10.1111/j.1556-4029.2012.02075.x>.
- Hammer, Ø., Harper, D., Ryan, P., 2001. PAST-Paleontological statistics 25 (7) uv. es/~pardomv/pe/2001_1/past/pastprog/past.pdf, acessado em.
- Hayes, S., 2016a. Faces in the Museum: revisiting the museum of facial reconstructions. *Mus. Manag. Curatorsh.* 31 (3), 218–245. <https://doi.org/10.1080/09647775.2015.1054417>.
- Hayes, S., 2016b. A geometric morphometric evaluation of the Belanglo 'Angel' facial approximation. *Forensic Sci. Int.* 268 (Supplement C), e1–e12. <https://doi.org/10.1016/j.forsciint.2016.09.009>.
- Hayes, S., Milne, N., 2011. What's wrong with this picture? An experiment in quantifying accuracy in 2D portrait drawing. *Vis. Commun.* 10 (2), 149–174. <https://doi.org/10.1177/1470357211398442>.
- Hayes, S., Valentin, F., Buckley, H., Spriggs, M., Bedford, S., 2009. Faces of the Teouma Lapita people: art, accuracy and facial approximation. *Leonardo* 42 (3), 284–285. <https://doi.org/10.1162/leon.2009.42.3.284>.
- Hayes, S., Shoocongdej, R., Pureepatpong, N., Sangvichien, S., Chintakanon, K., 2017. A Late Pleistocene woman from Tham Lod, Thailand: the influence of today on a face from the past. *Antiquity* 91 (356), 289–303. <https://doi.org/10.15184/aqy.2017.18>.
- Hayes, S., McDonald, H., Jastkowiak, S., Gay, G., 2019. *Predictive accuracy of Estimating Facial Appearance from the Skull: the Belanglo 'Angel' 7th Unfamiliar Face Identification Group Conference*, vols. 7–8. University of New South Wales, Sydney Australia. February, 2019).
- Huang, X., Xia, Z.-Y., Bin, X., He, G., Guo, J., Adnan, A., Yin, L., Huang, Y., Zhao, J., Yang, Y., 2022. Genomic insights into the demographic history of the Southern Chinese. *Frontiers in Ecology and Evolution* 10, 853391. <https://doi.org/10.3389/fevo.2022.853391>.
- Hudjashov, G., Endicott, P., Post, H., Nagle, N., Ho, S.Y., Lawson, D.J., Reidla, M., Karmin, M., Rootsi, S., Metspalu, E., 2018. Investigating the origins of eastern Polynesians using genome-wide data from the Leeward Society Isles. *Sci. Rep.* 8 (1), 1823. <https://doi.org/10.1038/s41598-018-20026-8>.
- Kim, S.-R., Lee, K.-M., Cho, J.-H., Hwang, H.-S., 2016. Three-dimensional prediction of the human eyeball and canthi for craniofacial reconstruction using cone-beam computed tomography. *Forensic Sci. Int.* 261, 164.e161–164.e168. <https://doi.org/10.1016/j.forsciint.2016.01.031>.
- Kyllonen, K.M., Monson, K.L., 2020. Depiction of ethnic facial aging by forensic artists and preliminary assessment of the applicability of facial averages. *Forensic Sci. Int.* 313, 110353. <https://doi.org/10.1016/j.forsciint.2020.110353>.
- Larrabee, W., Makielski, K., 1993. *Surgical Anatomy of the Face*. Raven.
- Lipson, M., Skoglund, P., Spriggs, M., Valentin, F., Bedford, S., Shing, R., Buckley, H., Phillip, I., Ward, G.K., Mallick, S., Rohland, N., Broomandkoshbacht, N., Cheronet, O., Ferry, M., Harper, T.K., Michel, M., Oppenheimer, J., Sirak, K., Stewardson, K., Reich, D., 2018. Population turnover in remote Oceania shortly after initial settlement. *Curr. Biol.* 28 (7), 1157–1165. e1157. <https://doi.org/10.1016/j.cub.2018.02.051>.
- Lipson, M., Spriggs, M., Valentin, F., Bedford, S., Shing, R., Zinger, W., Buckley, H., Petchey, F., Matanik, R., Cheronet, O., Rohland, N., Pinhasi, R., Reich, D., 2020. Three phases of ancient migration shaped the ancestry of human populations in Vanuatu. *Curr. Biol.* 30 (24), 4846–4856. e4846. <https://doi.org/10.1016/j.cub.2020.09.035>.
- Liu, Y.-C., Hunter-Anderson, R., Cheronet, O., Eakin, J., Camacho, F., Pietrusewsky, M., Rohland, N., Ioannidis, A., Athens, J.S., Douglas, M.T., 2022. Ancient DNA reveals five streams of migration into Micronesia and matrilocality in early Pacific seafarers. *Science* 377 (6601), 72–79. <https://doi.org/10.1126/science.abc6536>.
- Mala, P.Z., 2013. Pronasale position: an appraisal of two recently proposed methods for predicting nasal projection in facial reconstruction. *J. Forensic Sci.* 58 (4), 957–963. <https://doi.org/10.1111/1556-4029.12128>.
- Mala, P.Z., Velemínska, J., 2016. Vertical lip position and thickness in facial reconstruction: a validation of commonly used methods for predicting the position and size of lips. *J. Forensic Sci.* 61 (4), 1046–1054. <https://doi.org/10.1111/1556-4029.13064>.
- Needham, C., 2002. *Drawing the Past: Reconstructing the Visual Manifestations of Disease and Trauma from Archaeological Human Remains*. M Phil, University of Manchester, Manchester.
- O'Higgins, P., Jones, N., 1998. Facial growth in *Cercopithecus torquatus*: an application of three dimensional geometric morphometric techniques to the study of morphological variation. *J. Anat.* 193, 251–272. <http://hymms.fme.googlepages.com/resources>.
- O'Higgins, P., Jones, N., 2006. Tools for Statistical Shape Analysis. Hull York Medical School. <http://hymms.fme.googlepages.com/resources>.
- O'Toole, A.J., Price, T., Vetter, T., Bartlett, J.C., Blanz, V., 1999. 3D shape and 2D surface textures of human faces: the role of "averages" in attractiveness and age. *Image Vis. Comput.* 18 (1), 9–19. [https://doi.org/10.1016/S0262-8856\(99\)00012-8](https://doi.org/10.1016/S0262-8856(99)00012-8).
- Pietrusewsky, M., 1996. The Physical Anthropology of Polynesia: a Review of Some Cranial and Skeletal Studies. *Oceanic Culture History: Essays in Honour of Roger Green*. New Zealand Journal of Archaeology Special Publication, Wellington, pp. 343–353.
- Posth, C., Nägele, K., Collieran, H., Valentin, F., Bedford, S., Kami, K.W., Shing, R., Buckley, H., Kinaston, R., Walworth, M., 2018. Language continuity despite population replacement in Remote Oceania. *Nature ecology & evolution* 2 (4), 731–740. <https://doi.org/10.1038/s41559-018-0498-2>.
- Prag, J., Neave, R., 1997. *Making Faces: Using Forensic and Archaeological Evidence*. British Museum Press.
- Richmond, S., Howe, L.J., Lewis, S., Stergiakouli, E., Zhurov, A., 2018. Facial genetics: a brief overview. *Front. Genet.* 9, 462. <https://doi.org/10.3389/fgene.2018.00462>.
- Rohlf, F.J., 2015. The tps series of software. *Hystrix* 26 (1), 9–12.
- Rynn, C., 2007. *Craniofacial approximation and Reconstruction: Tissue Depth Patterning and the Prediction of the Nose* [PhD]. The University of Dundee, Dundee.
- Rynn, C., Wilkinson, M., Peters, H., 2010. Prediction of nasal morphology from the skull. *Forensic Sci. Med. Pathol.* 6 (1), 20–34. <https://doi.org/10.1007/s12024-009-9124-6>.
- Sadick, N.S., Bosniak, S.L., Cantisano-Zilkha, M., Glavas, I.P., Roy, D., 2007. Definition of the tear trough and the tear trough rating scale. *J. Cosmet. Dermatol.* 6 (4), 218–222. <https://doi.org/10.1111/j.1473-2165.2007.00336.x>.
- Salvador-Amores, A., 2016. Afterlives of dean C. Worcester's colonial photographs: visualizing igorot material culture, from archives to anthropological fieldwork in northern Luzon. *Vis. Anthropol.* 29 (1), 54–80. <https://doi.org/10.1080/08949468.2016.1108832>.
- Sarilita, E., Rynn, C., Mossey, P.A., Black, S., Oscandar, F., 2017. Nose profile morphology and accuracy study of nose profile estimation method in Scottish subadult and Indonesian adult populations. *Int. J. Leg. Med.* 132 (3), 1–9. <https://doi.org/10.1007/s00414-017-1758-4>.
- Sheppard, P., 2019. Early Lapita Colonisation of Remote Oceania: an Update on the Leapfrog Hypothesis. ANU Press, Canberra. <https://doi.org/10.22459/TA52.2019>.
- Skoglund, P., Posth, C., Sirak, K., Spriggs, M., Valentin, F., Bedford, S., Clark, G., Reepmeyer, C., Petchey, F., Fernandes, D., Fu, Q., Harney, E., Lipson, M., Mallick, S., Novak, M., Rohland, N., Stewardson, K., Abdullah, S., Cox, M., Reich, D., 2016. Genomic insights into the peopling of the southwest pacific. *Nature* 538 (7626), 510–513. <https://doi.org/10.1038/nature19844>.
- Spriggs, M., 1997. *The Island Melanesians*. Blackwell.
- Stephan, C.N., 2002. Facial approximation: globe projection guideline falsified by exophthalmometry literature. *J. Forensic Sci.* 47 (4), 730–735. <https://www.ncbi.nlm.nih.gov/pubmed/12136981>.
- Stephan, C.N., 2003. Facial approximation: an evaluation of mouth-width determination. *Am. J. Phys. Anthropol.* 121 (1), 48–57. <https://doi.org/10.1002/ajpa.10166>.
- Stephan, C.N., 2017. 2018 tallied facial soft tissue thicknesses for adults and sub-adults. *Forensic Sci. Int.* 280, 113–123. <https://doi.org/10.1016/j.forsciint.2017.09.016>.
- Stephan, C., Davidson, P.L., 2008. The placement of the human eyeball and canthi in craniofacial identification. *J. Forensic Sci.* 53 (3), 612–619. <https://doi.org/10.1111/j.1556-4029.2008.00718.x>.
- Stephan, C.N., Simpson, E.K., 2008. Facial soft tissue depths in craniofacial identification (part 1): an analytical review of the published adult data. *J. Forensic Sci.* 53 (6), 1257–1272. <https://doi.org/10.1111/j.1556-4029.2008.00852.x>.
- Stephan, C.N., Huang, A.J.R., Davidson, P.L., 2009. Further evidence on the anatomical placement of the human eyeball for facial approximation and craniofacial superimposition. *J. Forensic Sci.* 54 (2), 267–269. <https://doi.org/10.1111/j.1556-4029.2008.00982.x>.
- Stewart, T., 1983. The points of attachment of the palpebral ligaments: their use in facial reconstructions on the skull. *J. Forensic Sci.* 28 (4), 858–863. <https://doi.org/10.1520/JFS11592J>.
- Taylor, K.T., 2001. *Forensic Art and Illustration*. CRC Press.
- Utsumo, H., Kageyama, T., Uchida, K., Kibayashi, K., Sakurada, K., Uemura, K., 2016. Pilot study to establish a nasal tip prediction method from unknown human skeletal

- remains for facial reconstruction and skull photo superimposition as applied to a Japanese male populations. *Journal of Forensic and Legal Medicine* 38, 75–80. <https://doi.org/10.1016/j.jflm.2015.11.017>.
- Valentin, F., Détroit, F., Spriggs, M.J., Bedford, S., 2016. Early Lapita skeletons from Vanuatu show polynesian craniofacial shape: implications for remote oceanic settlement and Lapita origins. *Proc. Natl. Acad. Sci. USA* 113 (2), 292–297. <https://doi.org/10.1073/pnas.1516186113>.
- Valentin, F., Clark, G., Parton, P., Reepmeyer, C., 2020. Mortuary practices of the first Polynesians: formative ethnogenesis in the Kingdom of Tonga. *Antiquity* 94 (376), 999–1014. <https://doi.org/10.15184/aqy.2020.89>.
- Vandermeulen, D., Claes, P., De Greef, S., Willems, G., Clement, J., Suetens, P., 2012. Automated Facial Reconstruction. *Craniofacial identification*, p. 203.
- Webster, M., Sheets, H.D., 2010. A practical introduction to landmark-based geometric morphometrics. *Quantitative Methods in Paleobiology* 16, 168–188.
- Wilkinson, C., 2004. *Forensic Facial Reconstruction*. Cambridge University Press.
- Wilkinson, C., Mautner, S.A., 2003. Measurement of eyeball protrusion and its application in facial reconstruction. *J. Forensic Sci.* 48 (1), 12–16. <https://www.ncbi.nlm.nih.gov/pubmed/12570193>.
- Wilkinson, C., Motwani, M., Chaing, E., 2003. The relationship between the soft tissues and the skeletal detail of the mouth. *J. Forensic Sci.* 48 (4), 728–732.
- Wong K, F., 2004. Entanglements of ethnographic images: Torii Ryūzō's photographic record of Taiwan aborigines (1896–1900). *Jpn. Stud.* 24 (3), 283–299. <https://doi.org/10.1080/10371390412331331546>.
- Yang, M.A., Fan, X., Sun, B., Chen, C., Lang, J., Ko, Y.-C., Tsang, C.-h., Chiu, H., Wang, T., Bao, Q., 2020. Ancient DNA indicates human population shifts and admixture in northern and southern China. *Science* 369 (6501), 282–288. <https://doi.org/10.1126/science.aba0909>.